ExpM+NF: Differentially Private Machine Learning that Surpasses DPSGD

Robert A. Bridges*, Vandy J. Tombs*, Christopher B. Stanley

Oak Ridge National Laboratory, Oak Ridge, TN

{bridgesra, tombsvj, stanleycb} @ornl.gov

Abstract-In this pioneering work we formulate ExpM+NF, a method for training machine learning (ML) on private data with pre-specified differentially privacy guarantee $\varepsilon > 0$, $\delta = 0$, by using the Exponential Mechanism (ExpM) and an auxiliary Normalizing Flow (NF). We articulate theoretical benefits of ExpM+NF over Differentially Private Stochastic Gradient Descent (DPSGD), the state-of-the-art (SOTA) and de facto method for differentially private ML, and we empirically test ExpM+NF against DPSGD using the SOTA implementation (Opacus [1] with PRV accounting) in multiple classification tasks on the Adult Dataset (census data) and MIMIC-III Dataset (electronic healthcare records) using Logistic Regression and GRU-D, a deep learning recurrent neural network with ~20K-100K parameters. In all experiments, ExpM+NF achieves greater than 93% of the non-private training accuracy (AUC) for $\varepsilon \in [1e-3, 1]$, exhibiting greater accuracy (higher AUC) and privacy (lower ε with $\delta = 0$) than DPSGD. Differentially private ML generally considers $\varepsilon \in [1, 10]$ to maintain reasonable accuracy; hence, ExpM+NF's ability to provide strong accuracy for orders of magnitude better privacy (smaller ε) substantially pushes what is currently possible in differentially private ML. Training time results are presented showing ExpM+NF is comparable to (slightly faster) than DPSGD. Code for these experiments will be provided after review. Limitations and future directions are provided.

Index Terms—differential privacy, machine learning, exponential mechanism, normalizing flows, optimization

1. Introduction

As collection and storage of data on individuals and entities becomes more frequent and detailed, rigorous methods for ensuring privacy of machine learning (ML) models trained on sensitive data is a pressing need. Examples from diverse domains are easy to find including predictive models for: advanced diagnosis and treatment using healthcare records and images [2, 3], increased security of IOT devices [4], and enabling smart meters to help transition to a carbon-free energy grid [5], to name a few.

Winning the 2017 Gödel prize, differential privacy (DP) is a widely accepted standard for privacy preserving analytics that has been adopted by the 2020 US Census [6], Apple [7], Google [8], Microsoft [9] and a myriad of research applications [10]. DP masks private data by injecting randomness into an algorithm, often at the expense of accuracy. In particular, DP admits provable quantifiable limits—in terms of a privacy budget (ε, δ) —on the possible inferences an outsider can make about the private data when viewing the results of the analytics.

In this paper, we present ExpM+NF, a fundamentally different approach for achieving differentially private ML, by which we mean training an ML algorithm on a single (private) dataset with a DP guarantee. Our method leverages the Exponential Mechanism (ExpM) [11], a well-established DP technique for optimizing a utility (inverse loss) function. The process is to sample from the ExpM distribution, a probability distribution over the model's parameter space (the domain of the utility/loss function) so that near-optimal (resp., far-from-optimal) parameters have high (resp., low) likelihood. By design, sampling from this distribution produces, with high likelihood, near-optimal parameters that are furnished with a strong privacy guarantee—the privacy budget $\varepsilon>0$ is pre-specified and $\delta=0$.

While ExpM is well known, two obstructions prevented its prior use in ML applications. First, sampling from the requisite distribution is intractable except for finite or otherwise very simple sample domains, where ExpM reduces to sampling from a multinomial. Examples of using ExpM for differentially private ML in the finite setting exist, e.g.: [12] (private decision tree with only categorical features), [13] (private PCA), and [14] (private feature selection with only categorical variables). Notwithstanding these examples, ExpM is historically intractable in most ML applications as the optimization is of a loss function over continuous parameter space [15–18]. Secondly, an a priori bound on sensitivity must be proven for the given utility (equiv., loss) function, which is difficult in general, e.g., see [17].

To address the first barrier, we leverage an auxiliary Normalizing Flow (NF) model—a deep learning model—that permits sampling from the otherwise intractable ExpM

^{*}Both authors contributed equally.

Research sponsored by the Laboratory Directed Research and Development Program of Oak Ridge National Laboratory, managed by UT-Battelle, LLC, for the U. S. Department of Energy. This manuscript has been co-authored by UT-Battelle, LLC under Contract No. DE-AC05-00OR22725 with the US DOE. The United States Government retains and the publisher, by accepting the article for publication, acknowledges that the United States Government retains a non-exclusive, paid-up, irrevocable, worldwide license to publish or reproduce the published form of this manuscript, or allow others to do so, for United States Government purposes. The DOE will provide public access to these results of federally sponsored research in accordance with the DOE Public Access Plan (http://energy.gov/downloads/doe-public-access-plan).

Code containing experiments presented available at Redacted URL.

Special thanks to Adam Spanhaus and Vishakh Gopu for their wisdom in debugging PyTorch implementation issues, and to Cory Watson for making sure the big computers "just work".

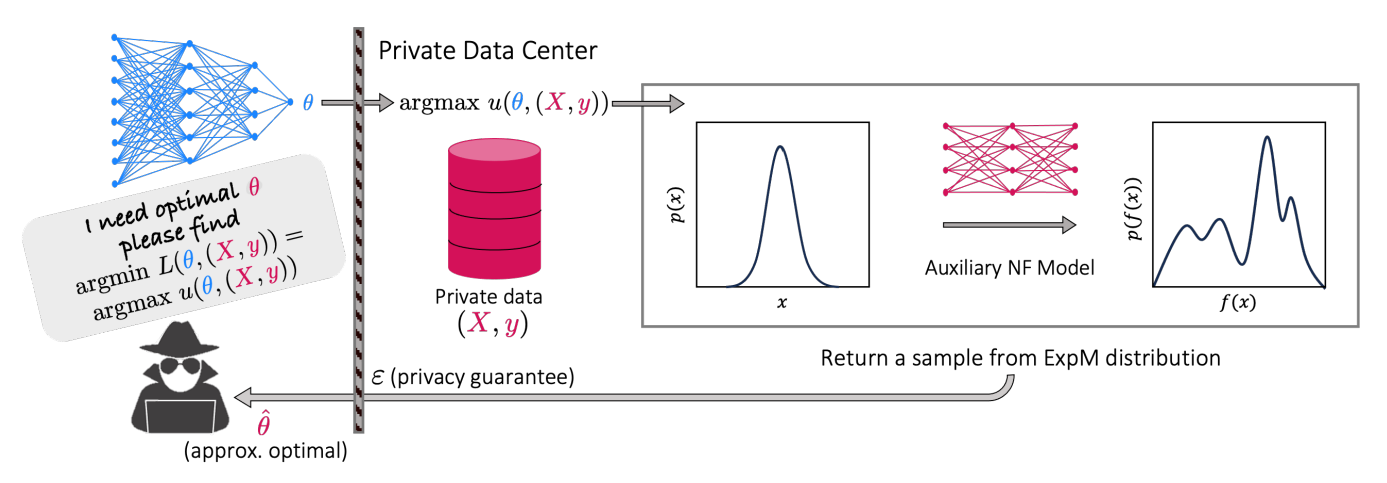


Figure 1: Figure depicts private data enclave on which outside entities would like to train a machine learning model. New technique, ExpM+NF, depicted at right, trains an auxiliary Normalizing Flow (NF) model to sample near optimal parameters from the otherwise intractable Exponential Mechanism (ExpM) density. Privacy parameters ($\varepsilon > 0$, $\delta = 0$) are prespecified by the private data center.

density [19]. For the second hurdle, by constraining our training to $\ell(2)$ (equiv. MSE) loss, we are able to bound sensitivity for supervised learning tasks with bounded targets (accommodating classification tasks via binary/one-hot encoding). The combined technique, ExpM+NF (see Figure 1), promises near optimal parameters and a strong privacy guarantee ($\varepsilon>0,\delta=0$) that is specified in advance by the user. Our hypothesis is that ExpM+NF attains better accuracy and privacy, simultaneously, than the current SOTA for differentially private ML.

Differentially private ML is currently achieved almost exclusively by a single, preeminent technique— Differentially Private Stochastic Gradient Descent (DPSGD) [20, 21]. DPSGD achieves a privacy guarantee by clipping and adding Gaussian noise to each gradient during SGD training. The many privacy guarantees (one per step) are collected into a single, overarching guarantee via composition theorems [20, 22-26]. In the conventional scenario of training ML on a single private dataset, one can see that DPSGD is wasteful by design-privacy is expended so that all gradients may be publicized, yet all that is required is the trained model. This leads to the overall privacy guarantee worsening with each step during training, of which hundreds to tens of thousands are usually needed. Once the privacy budget is expended, training must cease, perhaps prematurely. This has led to an unusable accuracyprivacy tradeoff in practice; e.g., accuracy results of Resnet-18 (model) on ImageNet (data) fall from 70% without privacy to under 20% with privacy ($\varepsilon = 2$) [27], and to quote Suriyakumar et al. [28] "DP learning algorithms are not well suited for off-the-shelf use in health care. First, DP models have significantly more severe privacy-utility tradeoffs in the MIMIC-III [electronic health records] setting, ..." Secondly, by expending privacy at each gradient step, DPSGD can only provide approximate DP, i.e., $\delta > 0$ (see Definition 1), a consequence of relying on composition theorems and, independently, of using Gaussian noise.

In contrast, our proposed method accommodates a sin-

gle pre-specified strong (i.e., not approximate) differential privacy guarantee ($\varepsilon>0, \delta=0$) that is achieved via a sample from the ExpM distribution. This avoids the step-wise decline in overall privacy as well as the use of the Gaussian Mechanism, and the application of advanced composition theorems, which necessitate $\delta>0$ (see Definition 1). By circumventing these drawbacks we hypothesize, and our results empirically confirm, that ExpM+NF admits stronger privacy and accuracy than is possible with DPSGD.

We present experiments using the Adult Dataset (US Census data) [29] and MIMIC-III data [30] (the preeminent electronic healthcare records dataset). We train a Logistic Regression (LR) model (~100 to 2.5K parameters) for both and for MIMIC, a modern deep learning recurrent neural network model called the Gated Recurrent Unit with Decay (GRU-D) [31] (~20K to 100K parameters) to compare ExpM+NF against the state-of-the-art implementation of DPSGD and their non-private baselines. Our experiments target high-priority domains for privacy.

Our results show that ExpM+NF achieves similar accuracy with orders of magnitude better privacy (lower ε with $\delta = 0$) than DPSGD in every experiment. More specifically, ExpM+NF achieves Area Under the ROC curve (AUC) of greater than 93% of the non-private baselines for ε as small as 1e-3 in every experiment—three to four orders of magnitude smaller than is considered in any similar previous work, and advancing the current standard that $\varepsilon \in [1, 10]$ is expected for ML [21]. This pushes what is possible in differentially private ML as the vast increase in the privacy budget may be used to address other hardships. For example, using basic composition one can afford to train hundreds, possibly thousands of ExpM+NF models, say with $\varepsilon_i \approx 1\mathrm{e}{-3}$ for hyperparameter tuning and still achieve a strong overall privacy guarantee, say $\varepsilon \approx 1$, today; or, to prevent anomalous training runs (e.g., bad randomized starting conditions) that can occasionally happen with a single model, one may release ten ExpM+NF models, each trained with $\varepsilon/10$ to be used in a voting scheme.

We note that our MIMIC-III non-private models reproduce previous works of Wang et al. [32], and our DPSGD implementations reproduce previous work of Suriyakumar et al. [28]. Although not an identical comparison (we cannot fully replicate these works without identical data and code), our non-private and DPSGD implementations exhibit greater or comparable accuracy and privacy than the previous works on these same datasets and learning tasks. By making our code public, we seek to set a reproducible benchmark for these learning tasks both in the private and non-private setting.

Limitations and future directions for advancing this promising method are discussed in Section 5. There are two primary limitations to ExpM+NF in this work. First, ExpM+NF requires a sensitivity bound for each loss function, and thus far we have only provided such a proof for $\ell(2)$ (equiv. mean squared error) loss. While this does not prove limiting in our experiments, future research is required for application to other loss functions. By comparison, DPSGD is readily applicable to theoretically any loss function. Secondly, ExpM+NF requires a completely different training regime (training an auxiliary NF model whose loss function depends the desired model and its loss function); hence, custom software engineering is currently required for use on each model architecture (e.g., on LR, GRU-D, ...). DPSGD comes professionally packaged in a PyTorch plugin, Opacus [1].

1.1. Background

Previous works on benchmark datasets and experiments with differentially private ML that lead to our work are discussed in our Experimental Methodology Section 3. Throughout, we denote the real numbers as \mathbb{R} . We will denote the universe from which datasets X, X' are drawn as D (so $X, X' \in D$) and use X, X' to denote neighboring datasets, meaning they are identical except for at most one data point (one row). The function $u: \Theta \times D \to \mathbb{R}$ will be a utility or scoring function we wish to maximize privately over Θ , the space of possible parameters for u. In the setting of machine learning, Θ is the space of parameters for the model; and we will use X, Y for the features and targets in lieu of simply X. Given loss function $L(X, Y, \theta)$, the utility is defined as $u := \phi \circ L$, with ϕ strictly decreasing, and usually $\phi(t) = -t$. The term "mechanism" simply means random function.

1.1.1. Differential Privacy. We begin by introducing when a mechanism is considered differentially private.

Definition 1 (Differential Privacy). A mechanism $f: \Theta \times D \to \mathbb{R}$ satisfies (ε, δ) -Differential Privacy or is (ε, δ) -DP if and only if

$$P(f(\theta, X) \in A) \le P(f(\theta, X') \in A)e^{\varepsilon} + \delta$$

for all neighboring $X, X' \in D, \theta \in \Theta, \varepsilon \geq 0$ and for all measurable sets A. When $\delta = 0$, we say f is ε -DP.

The ε term is an upper bound on the privacy loss. Intuitively, differential privacy measures how much an individual data point changes the output distribution of the mechanism f. If the mechanism's output is nearly identical in both cases (when any data point is or isn't included), meaning that ε is very small, then this is a privacy guarantee for any individual data point. This quantifies the intuitive notion that it is essentially indistinguishable if any one data point is included or not.

Approximate DP, or (ε, δ) -DP, provides a relaxed definition— δ is the probability that the mechanism f is not guaranteed to be ε -DP. This "probability of failure" interpretation has let many to suggest that δ should be no larger that 1/N where N is the number of data points in the dataset [33].

Differential privacy has many useful properties. First, post-processing is "free", meaning if $f(\theta, X)$ is (ε, δ) -DP, the same guarantee holds after composition with any function h; i.e., $h \circ f$ is also (ε, δ) -DP [33]. Secondly, it satisfies composition theorems; the most basic of which says that if f_1 and f_2 satisfy $(\varepsilon_1, \delta_1)$ -DP and $(\varepsilon_2, \delta_2)$ -DP, respectively, then $f_1 \circ f_2$ satisfies $(\varepsilon_1 + \varepsilon_2, \delta_1 + \delta_2)$ -DP [33]. The general problem of estimating the overall privacy bound (a single (ε, δ)) for a sequence of mechanisms $f_i(\theta_i, X), i = 1, ..., m$ each furnished with a privacy guarantee $(\varepsilon_i, \delta_i)$ -DP, is important for use. As the basic composition theorem above holds, it is not a tight bound (better estimates may exist), and hence, a large body of work [20, 22-26] provide advanced composition theorems (tradeoffs of ε and δ that depend on the ε_i, δ_i) that estimate this overall bound. Intuitively, as more information is released (as m grows), the overall privacy guarantee gets worse (ε and δ increase), and all advanced composition theorems entail an increase of δ for the better estimate of ε .

To achieve differential privacy in practice, randomness is leveraged. Determining how much randomness to inject requires understanding how sensitive the output of the mechanism is to different datasets.

Definition 2 (Sensitivity). The sensitivity of a mechanism $f: \Theta \times D \to \mathbb{R}$ is $\max |f(\theta, X) - f(\theta, X')|$ where the max is over neighboring $X, X' \in D, \theta \in \Theta$. We use s to denote an upper bound on sensitivity.

Once the sensitivity is determined, there are several DP mechanisms that have been shown to satisfy differential privacy. In this work, we utilize the exponential mechanism.

Definition 3 (Exponential Mechanism). For data $X \in D$ and a utility function $u: \Theta \times D \to \mathbb{R}$ with sensitivity s, the Exponential Mechanism (ExpM) returns $\theta \in \Theta$ with likelihood $p_{ExpM}(\theta; X) \propto \exp(\varepsilon u(\theta, X)/(2s))$.

A needed theorem shows ExpM satisfies differential privacy.

Theorem 1 ([11, 33]). The Exponential Mechanism (ExpM) i.e., sampling $\theta \sim p_{ExpM}(\theta, X) \propto \exp(\varepsilon u(\theta, X)/(2s))$ where utility function u has sensitivity s, provides ε -DP.

The original treatment of ExpM [11] furnishes utility

theorems—rigorous guarantees that bound how far ExpM samples can be from the optima.

1.1.2. Differentially Private Machine Learning. Differentially Private Stochastic Gradient Descent (DPSGD) is the predominant method for achieving differential privacy in machine learning models [21]. Algorithm 1 in [20] describes how the gradient for each data point (not batch) is clipped and Gaussian noise is added according a predefined noise scale. Clipping the gradient is necessary to ensure a bound on the sensitivity of the learning algorithm. The original DPSGD work also introduces the Moments Accountant as a method for approximating the privacy bound ε given some δ . The Moments Accountant relies on advanced composition theorems and noticing that the privacy bound is improved due to training in batches (i.e., subsampling the data) to tighten the upper bound on the privacy budget ε .

Following their work, there have been several privacy accounting methods proposed for DPSGD. One worth highlighting is the RDP Accounting method that computes the Renyi-DP, a relaxed definition of (ε,δ) -DP from which an (ε,δ) -DP bound can be computed. The RDP Accountant produces a tighter bound on the privacy budget than the Moments Accountant.

Gopi et al. in [26] later noted that for each iteration of training, there is a privacy curve δ_i over ε and that it is non-trivial to determine how to compose these to produce a single privacy curve for the entire training procedure. Based on prior work, they propose the PRV Accountant method that utilizes the privacy random variable (PRV) and Fast Fourier Transform to compose the privacy curves to arbitrary accuracy. This method introduces an error term for both ε and δ . They also show that the RDP Accounting method significantly overestimates the true value of ε . It's worthwhile to note that since the PRV Accounting method was only recently developed, the prior state-of-the-art results on MIMIC III used DPSDG with the RDP accounting method.

We note that objective perturbation, whereby one adds noise to the objective (loss) function, has been proposed for differentially private ML [16, 34], yet previous works on which we build, namely Suriyakumar et al. [28], report DPSGD is superior to objective perturbation. For a survey of differentially private ML, see Ji et al. [16] and Ponomareva et al. [21]

1.1.3. Normalizing Flows. We reference readers to the survey of Normalizing Flow (NF) research by Papamakarios et al. [19]. An NF model is a neural network, $g=g_k\circ...\circ g_1:\mathbb{R}^n_z\to\mathbb{R}^n_\theta$, with each layer $g_i:\mathbb{R}^n\to\mathbb{R}^n$, called a flow, that is invertible and differentiable. We let θ_{NF} denote the parameters of g to be learned, and suppress this notation for simplicity unless needed. Notably, g (and by symmetry, g^{-1}) preserves probability densities: if p_z is a probability density, then $\theta\mapsto p_z(g^{-1}(\theta))|{\rm det}\,J_{g^{-1}}(\theta)|$ is also, which is proven by the change of variables induced by $\theta=g(z)$.

Let p_{θ}^* be an intractable target density over \mathbb{R}^n (meaning p_{θ}^* can be computed up to a constant factor, but we cannot sample from p_{θ}^*), in our case $p^* = p_{ExpM}$. Let p_z be a

tractable density also over \mathbb{R}^n , especially, p_z is Gaussian. Then g can be trained to transform p_z into p_θ so that $p_\theta \approx p_\theta^*$ as follows: iteratively sample a batch $z_i \sim p_z, i=1,...,N$ and minimize the empirical KL divergence of the base density p_z with the pull-back of the target density, namely $p_\theta^*(g(z))|\det J_g(z)|$; that is, minimize "Reverse KL" (RKL) loss.

$$KL(p_z(z), p_{\theta}^*(g(z))|\det J_g(z)|) \cong \frac{1}{N} \sum_{i=1}^N \log \frac{p_z(z_i)}{p_{\theta}^*(g(z_i))|\det J_g(z_i)|} . \tag{1}$$

Once trained, $\theta = g(z)$ with $z \sim p_z$ gives approximate samples from previously intractable p_{θ} !

What is needed to compute this loss function is efficient computation of, first, the target density $p_{\theta}^*(\theta)$, and second, the log determinant Jacobian term $\log |\det J_g|$. Generally, NFs are designed to make computing this log determinant computationally feasible (e.g., using flows g_i so that J_g is triangular or that satisfy Theorem 2) while balancing the expressiveness.

In this work, we leverage the Planar Flows of Rezende & Mohamed [35] and their more expressive generalization, Sylvester Flows [36]. Let $z \in \mathbb{R}^d$, $A(d \times m)$, $B(m \times d)$, $c \in \mathbb{R}^m$, and $h : \mathbb{R} \to \mathbb{R}$ an activation function that we ambiguously apply to vectors componentwise $(h(\vec{v}) = [h(v_1), ..., h(v_d)]^t)$.

Definition 4 (Sylvester Flow). A Sylvester flow is defined as g(z) = z + Ah(Bz + c), and note that $J_g(z) = I_d + A_{d \times m} diag(h'(Bz + c))_{m \times m} B_{m \times d}$.

Theorem 2 (Sylvester a.k.a. Weinstein–Aronszajn Theorem). $\det(I_d + A_{d \times m} B_{m \times d}) = \det(I_m + B_{m \times d} A_{d \times m}).$

It follows that when m < d, we can compute the determinant, $J_q(z)$ in the lower dimensional representation!

Definition 5 (Planar Flow). A planar flow is a special case of a Sylvester flow when m = 1, so $A, B \in \mathbb{R}^d$.

Following Berg et al. [36], a Sylvester Flow can be implemented by using the special case where $A=Q_{d\times d}R_{d\times m}$ and $B=\hat{R}_{m\times d}Q_{d\times d}^t$ with Q orthogonal and R,\hat{R} upper triangular. (This is a restriction in that it uses the same Q for both A,B). To instantiate an orthogonal matrix Q, we define unit vectors v and set $Q:=\prod_v I-2vv^t$ which is a product of Householder reflections. A well know fact is that Householder reflections are orthogonal, and any orthogonal matrix is as a product of Householder reflections [37]. Note this is obviated in the Planar Flow case since A,B are simply d-dimensional vectors.

2. ExpM+NF Method

Figure 1 depicts the setting that we will consider: a private data enclave that wishes to permit optimization on their data; in particular, training and publicly releasing an ML algorithm on that data. Fitting an ML model on training features and targets (X,Y) constitutes finding parameters

 θ that minimizes a loss function $L(X,Y,\theta)$, and ExpM requires specifying a utility function $u(X, Y, \theta)$ to be maximized in θ . Therefore, we will set $u = \phi \circ L$ for strictly decreasing ϕ . Throughout our experiments we use u = -L, but provide insights into choosing ϕ in Section 2.1.

The approximately optimal parameters θ are found by sampling

$$\theta \sim p_{ExpM}(\theta) \propto \exp[u(X, Y, \theta)\varepsilon/2s]$$

furnishing an ε -DP guarantee. Importantly, the privacy parameter ε is pre-specified. To define the density, we must identify the sensitivity bound s (Defn. 2). When s is large, it diminishes the influence of u, and reduces accuracy by increasing the variance of the sampled θ .

For application of our method we must first find an ideally tight bound s on the sensitivity of the utility function u. Since u, s are intimately tied to the loss function L, this up-front task is generally required per loss function and can depend on the model outputs. In this initial work, we consider $\ell(2)$ loss functions $(\sum_{X,Y} (\hat{y}(x)-y)^2)$ on classification tasks with model outputs and targets bounded by 1 giving s = 1; for more details see Section 2.2.

The last step is to sample $\theta \sim p_{ExpM}(\theta)$. This step replaces an SGD scheme but fills the same role-it produces approximately optimal parameters for the ML model. Unfortunately, p_{ExpM} is a historically intractable density for non-finite domains, so sampling directly is infeasible in most supervised learning applications. Our new approach trains an auxiliary NF model (see Section 1.1.3) to transform a Gaussian base density p_z into our target density $p_{\theta}^* := p_{ExpM}$. As we discussed when introducing NFs (Section 1.1.3), the Reverse KL loss function, given by Equation 1, only requires computing the determinant Jacobian term (made tractable by the design of the NF) and $\log p_{ExpM}$ up to any positive constant, which is simply $u\varepsilon/2s$, essentially computing our loss function. In short, the NF training is computationally well suited for approximating the ExpM density. In this work, the NF models will utilize Planar and Sylvester Flows, introduced in Section 1.1.3. Finally, once a sample is produced from the trained NF, it can be released with the ε -DP guarantee, allowing use of the trained model.

Algorithm 1 outlines the basic method for producing a differentially private ML model with ExpM+NF, which entails training an auxiliary NF model to allow for approximate sampling from the ExpM and will give the ML model parameters with an ε -DP guarantee. Variants of this general setup may be pursued in use.

2.1. Choosing $u = \phi \circ L$

While any strictly decreasing ϕ theoretically ensures identical optimization, in practice ϕ must separate the nearoptimal θ from those that are far from optimal. This means the derivative must be a sufficiently large negative value over an appropriate range of $L(\theta)$ to discriminate high versus low utility θ . In particular, using a negative sigmoid function, which is flat $(\phi' \approx 0)$ except in a limited neighborhood, is

Algorithm 1 Differentially Private ML with Exp+NF

Input: Training set (X,Y), a base distribution p_z , a loss function L, decreasing ϕ , privacy budget ε , sensitivity bound s.

Initialize $\theta_{NF,0}$ randomly

for t in T do

Generate N samples from base distribution for each $i \in [N]$, $z_i \sim p_z$

Produce N parameter samples & Jacobian for each $i \in [N]$,

 $\theta_i = g_{\theta_{\text{NF},t}}(z_i)$ $\log |\det J_g(z_i)|$ (depends on NF)

Compute utility for each parameter sample for each $i \in [N]$, $u(X, Y, \theta_i) = \phi \circ L(X, Y, \theta_i)$

Evaluate log of target probability of samples

log
$$p_{\theta}^*(\{\theta_i\}) = \frac{\varepsilon}{2s} \sum_{i=1}^N u(X,Y,\theta_i)$$

Compute Reverse KL Loss using Eq. 1

 $\mathcal{L} = KL[p_z(z_i), p_\theta^*(\theta_i)|\det J_q(z_i)|]$

Update NF Model

 $\theta_{ ext{NF},t+1} = \theta_{ ext{NF},t} - \eta_t
abla_{ heta_{ ext{NF},t}} \mathcal{L}$

end for

sample from base distribution, $z \sim p_z$

Output ML model parameters, $\theta = g_{\theta_{NF,T}}(z)$ and ε privacy guarantee

unwise, unless we know which range of $L(\theta)$ will contain the optimal values a priori and shift ϕ to discriminate these values. Lastly, we note that choice of ϕ effects the sensitivity, and therefore may be designed to assist in producing the required sensitivity bound.

2.2. Bounding Sensitivity

Define the utility to be the negative loss so

$$u = -L = \sum_{(x,y)\in(X,Y)} l(x,y,\theta) + r(\theta)$$

where $l(x, y, \theta)$ is the loss from data point (x, y), and $r(\theta)$ is a regularization function. For two neighboring datasets (X,Y),(X',Y'), let $(x,y)\in (X,Y)$ and $(x',y')\in$ (X',Y') denote the lone row of values that are not equal. We obtain $|u(X, Y, \theta) - u(X', Y', \theta)| = |l(x, y, \theta) - l(x', y', \theta)|$; hence, bounding s is achieved by Lipschitz or $\ell(\infty)$ conditions on the per-data-point loss function l. Notably, regularization r does not affect sensitivity.

Theorem 3 (Sensitivity bound for $\ell(2)$ loss). Suppose our targets and model outputs reside in [0,1]. If u = -L = $-\sum_{(x,y)}(\hat{y}(x,\theta)-y)^2$, then $s \leq 1$. In particular, $s \leq 1$ for classification tasks using binary/one-hot encoded targets and logistic/soft-max outputs with $\ell(2)$ loss and u = -L.

Proof. Since
$$\hat{y}(x,\theta), y \in [0,1]$$
 we see $(\hat{y}(x,\theta)-y)^2 \in [0,1]$ and $(\hat{y}(x,\theta)-y')^2 \in [0,1]$ so $|(\hat{y}(x,\theta)-y)^2-(\hat{y}(x',\theta)-y')^2|<1$.

2.3. Contrasting ExpM+NF with DPSGD

Training a model with DPSDG is quite similar to non-private training but has a few key differences. First, data is placed into batches for training according to a defined sampling ratio so the actual batch size will vary during training. Second, per example gradients must be clipped to have norm below some value C (the max_grad_norm variable). Finally, Gaussian noise with variance σC , where σ is the specified noise scale, is added to each gradient.

Once DPSGD has finished training, the resulting model comes with an (ε, δ) -DP guarantee that must be computed using an accounting method (see Section 1.1). The weaker notion of differential privacy arises due to DPSGD's reliance on the Gaussian mechanism [20, 26] and the composition theorems that the accountant uses to bound the privacy budget of the entire training process. Because DPSGD clips the pre-example gradients, the sensitivity of the training procedure is bounded. The privacy bound ε for DPSGD relies on the noise scale, the sampling ratio, the number of training steps and δ . We may choose a privacy budget prior to training by fixing all but one of these parameters and using them to solve for the unfixed parameter.

ExpM+NF, on the other hand, requires an entirely new training regime as we must training an auxiliary NF model to produce optimal parameters. As Algorithm 1 shows, this requires sampling N samples from the base distribution, pushing these samples through the normalizing flow model, computing the log determinant of the Jacobian and computing $L(X,Y,\theta_i)$ for each of the parameter samples θ_i .

Once the training of the NF model is complete, the desired private ML model parameters are produced by pushing a single sample from the base distribution through the NF model. These parameters come with the prespecified ε -DP guarantee. This method completely avoids the use of composition theorems for producing the privacy bounds and does not require the weaker notion of differential privacy as $\delta=0$. It does, however, require a sensitivity bound on the utility function, which for some utility functions may be non-trivial to prove.

Computationally, both DPSGD and ExpM+NF incur overhead when compared to non-private training and the computational requirements depend greatly on the architecture of the models and hyperparameter choices for each. During training, most of DPSGD's inefficiency is due to clipping each gradient, although some additional computation is needed for sampling and adding Guassian noise to each gradient. ExpM+NF requires training an auxiliary NF model where most of the inefficiency comes from needing to compute $L(X, Y, \theta_i)$ for each of the sampled parameters, θ_i . Discovering implementations that efficiently train the NF q and ensure gradients are tracked throughout the process was much of the research for this work, and we will provide code for these experiments upon acceptance. DPSGD also requires computing the privacy budget and different accounting methods have different computational overhead. The PRV Accountant method [26] requires an upper bound on the privacy budget which is usually found by using the RDP accountant. For Exp+NF the privacy budget is pre-specified and thus does not require computing. We present timing results comparing ExpM+NF, DPSGD, and non-private training in Section 4.3.

3. Experiments & Methodology

For all datasets, tasks, and models, we implement a non-private baseline, DPSGD and ExpM+NF trained private versions. For the non-private and DPSGD models, we provide results for both binary cross entropy loss (BCE) and $\ell(2)$ loss, as both are common for binary classification. For privacy methods, we vary ε to see the accuracy-privacy trade-off. Differentially private ML research generally considers $\varepsilon \in [1,10]$ [21], hence we present plots of $0.5 \le \epsilon \le 10$, and, investigate results for ε as low as $1\mathrm{e}{-4}$. All experiments are coded in PyTorch.

For DPSGD the usual hyperparameters (epochs, batch size, momentum, learning rate, and regularization parameter) function as usual. We use the PRV method of accounting via Opacus with clipping parameter, max_grad_norm = 1 [39, 40], δ = 1e-5, roughly the inverse of the number of training data points, as are standard, and delta_error set to $\delta/1000$ (default). We compute the noise_multiplier parameter, which governs the variance of the Gaussian noise added to each gradient, to achieve the target privacy (ε, δ) based on the number of gradient steps (epochs and batch_size parameters) and the gradient clipping parameter max_grad_norm. As mentioned in the background section, the PRV Accounting method introduces an error term for ε that bounds the error in the estimate of the privacy guarantee. Notably, eps_error =.01 is the default fidelity, and computations become too expensive or intractable for eps_error <.0001. Hence, given target epsilon $\bar{\varepsilon}$, we set eps_error to be as close as possible to $\bar{\varepsilon}/100$ within the range [.0001, .01].

Our NF models always use a Gaussian base distribution with $N(\vec{0}, \mathrm{diag}(\sigma^2))$, and we treat the constant σ^2 appearing on the diagonal of the covariance matrix as a hyperparameter. The number of flows and parameters of the Sylvester model (Section 1.1.3) are also hyperparameters. Lastly, our method has hyperparmeters for training that include: epochs, NF batch size (how many model parameters to sample from the NF for each KL loss computation), data batch size (number of training data points used in each KL loss computation), learning rate, momentum, and regularization parameter.

Data is split into a train/dev/test split that is stratified, preserving class bias in each partition. For each ε , we performed a randomized grid search of hyperparemeters fitting on the train set and testing on the dev set. The hyperparmeters were refined usually twice for a total of about 60-90 hyperparmeter train/dev runs; this same procedure is used for all training methods (ExpM+NF, DPSGD, non-private). Only those hyperparameters producing the best results on the dev set are used in final results–fitting on training plus dev partitions and validating on the never-before-used test set. While in practice, hyperparameter searching will entail

TABLE 1: Information on data, prediction tasks, and models used for experiments tabularized. LR denotes logistic regression.

Dataset	Prediction Task (class bias)	Models $(n_{\text{parameters}})$	$n_{ m rows}$	$n_{ m features}$
Adult [38]	Income, Binary (24.8%/75.2%)	LR (103 parameters)	45,222	102
MIMIC-III [30, 32]	ICU Mortality, Binary (07.4%/92.6%)	LR (2497 parameters), GRU-D (20K-100K parameters)	21,877	2,496
MIMIC-III [30, 32]	ICU Length of Stay, Binary (47.1%/52.9%)	LR (2497 parameters), GRU-D (20K-100K parameters)	21,877	2,496

a loss of privacy, we ignore accounting for this as our goal is to compare the best achievable accuracy and privacy of ExpM+NF, DPSGD, relative to the nonprivate baseline.

While batch normalization is commonplace in non-private deep learning, it is not directly portable to the private setting as z-normalization learned in training must be shipped with the model [40]; hence, we do not use batch normalization for our private models, but we do provide results with vs. without batch normalization where applicable, namely for the non-private GRU-D model, Table 4. Details of the hyperparmeters used for each model can be found in our code base and vary per experiment and privacy level ε .

In all binary classification tasks we use AUC as our accuracy metric. Starting conditions can lead to anomalously good/bad models for all methods (non-private, DPSGD, ExpM+NF). We present the median across ten models, each with different random seeds, to provide robustness to outliers. More specifically, for both DPSGD and nonprivate training with BCE and $\ell(2)$ loss, once hyperparameter searching is complete, we train ten non-private baseline models, each with a different random seed, and present the median AUC. The highest non-private median across the two loss functions is the considered the baseline for each dataset, task and appears as a dotted line in result plots. For ExpM+NF we train ten NFs using the best hyperparameters and produce 1,000 sampled parameter sets from each NF, for a total of 10,000 parameter sets. We instantiate the 10,000 resulting models, compute their AUC results, and compare the median to DPSGD and the non-private baseline. One may prefer to compute the median of the 1,000 AUCs per NF model (producing 10 median AUCs), and report the median of these medians. We have empirically verified that the results are nearly identical in our experiments.

While we cannot visualize the NF's output distribution, we can investigate the distribution of AUCs attained by ExpM+NF models for each ε parameters. We present box plots in which indicate the distribution's median (middle line), first (Q1) and third (Q3) quartiles (box), and extend 1.5 times the inner quartile range (Q1 - 1.5 IQR, Q3+ 1.5 IQR, whiskers). To see anomalous models arising from fortunate/unfortunate starting positions (different random seeds), we overlay each of the ten model's means.

3.1. Adult Dataset Experimental Design

The Adult Dataset [38] is a subset of 1994 census data. We drop rows that have missing values leaving 45,222 rows. The target column is binary, indicating whether the adjusted gross income is above/less or equal to \$50K. The class bias is approximately 24.8%/75.2%. Column fnlwgt gives the weight of each row (this

is not a feature as it provides the proportion of the population that has the same set of features), and gives a multiple in our loss function. Six columns are numeric columns (age, capital_loss, captial_gain, education_num, hours_per_week, fnlwgt); two are binary (sex and the target); and the remaining eight columns are categorical with more than two values. We have converted all binary categorical columns to numerical binary values $\{0,1\}$, and categorical columns with more than two values into one-hot encoding. After this preparation, we have 104 columns (102 features, 1 weights column, 1 target).

For this prediction task, we test LR with a bias term, which entails 103 parameters to be learned with privacy. We used RMSProp optimizer for all models (non-private logistic regression, DPSGD PRV, and NF) with this dataset, task. Our train/dev/test ratio is 64%/16%/20%.

3.2. MIMIC III Dataset Experimental Design

MIMIC-III [30] is a large, open, electronic health record (EHR) database covering a diverse group of critical care patients at a medical center from 2001-2012. Our experimental design follows a progression of research on MIMIC-III. Wang et al. [32] create benchmarks of needed healthcare predictive tasks from the MIMIC-III dataset, downloadable (from MIMIC-III v1.4, as all_hourly_data.h5) with the codebase [41]. We use the binary prediction task benchmarks ICU Mortality and ICU Length of Stay (> 3 days) from Wang et al.'s pipeline. These tasks differ only in target and share the feature set consisting of 104 measurement means per hour over a 24 hour period for 21,877 patients. Mortality is extremely imbalanced (07.4%/92.6%), while Length of Stay is balanced (47.1%/52.9%). We employ standardization (z-score normalization) for each feature, and it is applied independently per train/dev/test partition to prevent privacy issues.

As an example use of the ICU Mortality and Length of Stay benchmarks, Wang et al. also present results of non-private LR and GRU-D [31] models. Che et al. [31] introduce the Gated Recurrent Unit with Decay (GRU-D) model, a deep neural network for time series learning tasks. GRU-D interpolates between the last seen value and the global mean so censored (missing) data does not need to be imputed in advance. Additionally, the hidden units of the GRU are decayed to zero with learned decay per component, which allows features that should have short influence (e.g., heart rate) vs. long influence (e.g., dosage/treatment) to have learned rate of diminishing value. Wang et al. provide non-private results for LR and GRU-D models on these two tasks as well as implementations.

Suriyakumar et al. [28] replicate Wang et al.'s results on these two tasks for non-private baselines, then provide DPSGD (with RDP accountant) results as well. To the best of our knowledge, Suriyakumar et al. [28] present the state of the art in differentially private ML on these MIMIC-III benchmarks. Unfortunately, their code is not provided.

Using the currently available data (MIMIC-III v1.4, as all_hourly_data.h5), and following preprocessing code and descriptions of Wang et al. we replicate these benchmarks as closely as possible. Further, we implement the LR and GRU-D models with non-private and DPSGD with PRV accounting training as to compare against ExpM+NF. PRV accounting [26] provides a better privacy bound than RDP, and we present comparative results across the two accounting methods. There are discrepancies between our dataset and Suriyakumar et al.'s description of the data, possibly because MIMIC-III was updated. The current MIMIC-III ICU Mortality and Length of Stay benchmarks have 89.1% missingness rate and 104 features per hour \times 24 hours giving 2,496 columns. Suriyakumar et al. claim to have 78% missingness and only 78 features per hour, but they report the number of columns is reported as "24,69", seemingly a typo (if the correct is 2,496, would entail 104 feature per hour). The number of rows matches exactly. The LR models entails privately learning these 2,497 parameters. Like our Adult Dataset Experiment, we use RMSProp optimizer with a scheduler that reduces the learning rate for all LR models.

For GRU-D, we follow Suriyakurmar et al. [28] and when needed the original GRU-D work of Che et al. [31]. Suriyakumar et al. [28] used batch normalization (BN) even when training privately with DPSGD, but this has since been revealed as a source of privacy leakage [40]. Hence, we do not use BN with our DPSDG implementations, but we do train a non-private model both with and without BN applied to the top regressor layer. We apply a dropout layer to the top regressor layer, treating the dropout probability as a hyperparameter. Unlike [28], we treat the hidden size as a hyperparameter for all experiments. The main motivation for this choice was that memory constraints on the GPU hardware used to perform ExpM+NF required that we used a hidden size no larger than 10. For the non-private and DPSGD implementations, we allow the hidden size to vary between 10 and 100 for our randomized grid search, so this constraint was only limiting for our new method. For training non-privately and with DPSGD, we use the Adam optimization method and for the NF model we use RMSProp with a scheduler. This is our the best possible replication of Wang et al. and Suriyakurmar et al.'s experiments save the choice to omit batch normalization.

Notably, Che et al [31] also provide non-private GRU-D results on MIMIC-III data for an ICU Mortality prediction task. Since Che et al. do not follow the preprocessing of Wang et al. and specifically claim to use 48 hours of data (while we, Wang, Suriyakurmar use 24 hours), we do not consider their results comparable.

4. Experimental Results

We discuss results by experiment in the subsections below. In addition to the accuracy vs. privacy results per experiment, we include results on our NF model distributions, and DPSGD accounting methods.

4.1. Adult Dataset Results

Our hyperparameter search found that DPSGD needs very few epochs (usually under 25) and relatively small batch sizes. Given the small number of epochs no scheduler was used with DPSGD. For NF training and the nonprivate model, a scheduler was used with patience = 1000. We found that only 2-7 planar flows (see Section 5), on the order of 1,000 parameters, provided the best results.

Our nonprivate logistic model achieved similar results for both BCE and $\ell(2)$ loss, namely 91.82% and 91.93%, respectively. Figure 2 compares DPSGD, ExpM+NF, and the nonprivate baseline's median AUC across the ten models trained for each method and privacy parameter. DPSGD results show only slightly better results for BCE vs. $\ell(2)$ loss. Both experience a steady drop from about 98% of the non-private AUC at $\varepsilon=1$ to essentially random guessing at $\varepsilon=2.5\mathrm{e}{-4}.$

Our results show that ExpM+NF provides greater privacy and accuracy than DPSGD across the board, and ExpM+NF achieves greater than 98% of the non-private AUC for $\varepsilon \geq 2.5\mathrm{e}{-2}$ and greater than 93% of the nonprivate AUC for $\varepsilon \geq 5\mathrm{e}{-4}.$ ExpM+NF admits results for ε as low as 1e-6, the lowest we attempted, although results become essentially random for $\varepsilon = 1\mathrm{e}{-5}$ or less on this dataset, task. ExpM+NF median AUC for $\varepsilon=1\mathrm{e}{-1}$ and 1e-2 are anomalously low compared to results for neighboring ε values. Figure 3 visualizes the AUC distribution per ε using box plots with the ten NFs' means overlaid. We can see in Figure 3 that $\varepsilon = 1\mathrm{e}{-1}$ had two NF models whose mean was far lower than the others (two dots much lower than median), and $\varepsilon = 1\mathrm{e}{-2}$ experienced three such outlier NFs. All ten NFs for each ε had identical hyperparmeters, with the lone difference being the random seed. This leads us to believe that starting conditions can have a large effect on ExpM+NF's accuracy, and the randomness in the ten NF starts are seen in the results.

4.2. MIMIC III Results

Our work shows substantial improvement for differentially private ML on the previous works' health care prediction tasks [28, 32]. By using the PRV Accounting method, we achieve state-of-the-art for DPSGD with both LR and GRU-D models on both ICU Mortality and Length of Stay tasks. Further still, by using ExpM+NF we are able to outperform these new state-of-the-art DPSGD results. Table 2 displays experimental results for the ICU Mortality and Length of Stay task experiments with both LR and GRU-D.

In these experiments, ExpM+NF again exhibits greater than 93% of the non-private models' AUC for all $\varepsilon \geq 1\mathrm{e}{-3}$.

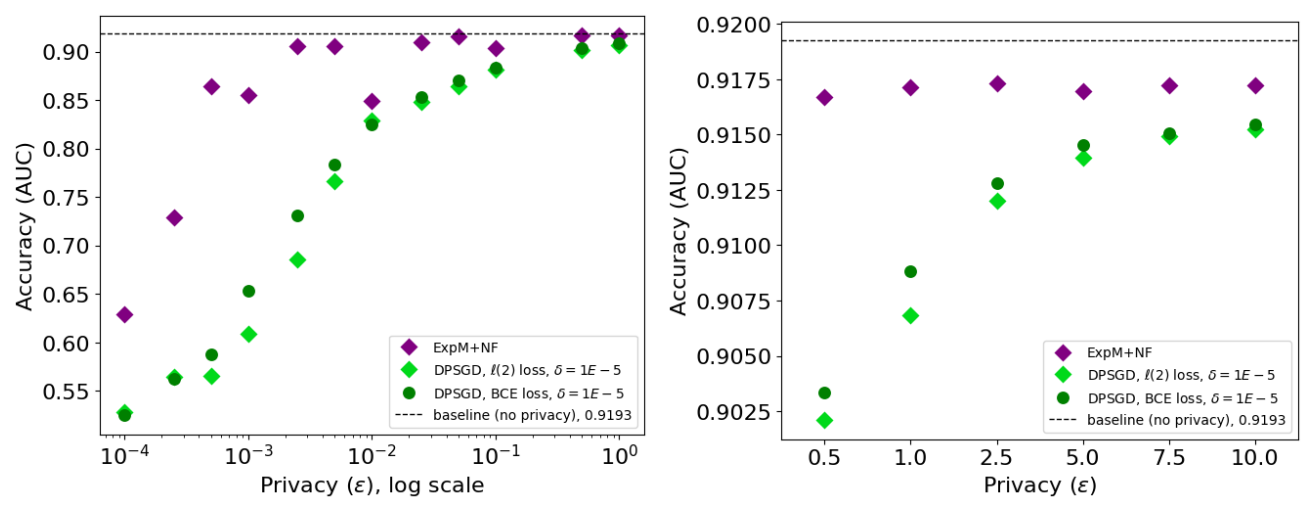


Figure 2: Adult Dataset Results - plots compare ExpM+NF, DPSGD, and nonprivate baseline models' median AUC results across ten models per ε . Left plot shows results for $\varepsilon \in [1e-4,1]$ (extremely strong to strong privacy) and **right plot** for $\varepsilon \in [1,10]$ (strong to weak privacy). ExpM+NF achieves greater accuracy than DPGSD for all ε and achieves greater than 93% of the non-private training for $\varepsilon \geq 5e-4$.

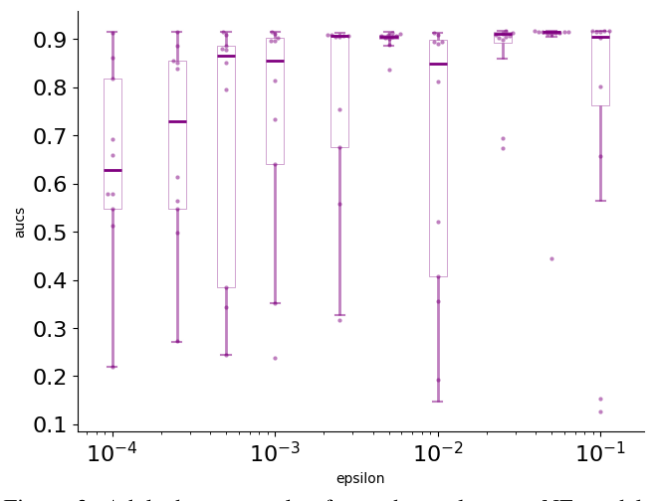


Figure 3: Adult dataset results, for each ε value, ten NF models are trained and used to produce 1,000 samples each from the ExpM distribution. We present box plots of the 10,000 resulting classifiers' AUC values. For each NF model's 1,000 samples we compute the mean AUC, which are overlayed as dots.

ExpM+NF surpasses DPSGD in all experiments except $\varepsilon \geq 2$ with LR model on the Length of Stay task, in which all privacy methods achieve 99% of the non-private model. Viewed through another lens, ExpM+NF maintains a greater AUC for $\varepsilon \geq 1\mathrm{e} - 3$ than DPSGD for $\varepsilon = 1, \delta = 1\mathrm{e} - 5$ in all MIMIC-III experiments, respectively. For both prediction tasks, the AUCs achieved by ExpM+NF of the GRU-D model are, for all $\varepsilon \geq 1\mathrm{e} - 3$, better than the non-private LR or GRU-D models' results reported by Suriyakumar [28]. These results shows that for both the simple LR model and the deep learning model GRU-D, Exp+NF substantially pushes the privacy-accuracy curve.

Our results show no significant difference in non-private or DPSGD trained models when using BCE vs. $\ell(2)$ loss. We found substantial limitations to the DPSGD RPD accountant compared to the SOTA accounting method, PRV. Our results show GRU-D, a much more expressive model than LR, does indeed surpass LR in AUC for non-private and each private training method in all experiments, respectively. This trend is seen in Che et al.[31] and Wang et al. [32], but results are the inverse (LR is more accurate) in results of Suriyakumar et al. [28].

We provide benchmark timing results for all three training methods. Our findings are that all private training methods are slower than non-private (expected), and that when including the time to compute the noise_multiplier, DPSGD is slower than ExpM+NF for both LR and GRU-D training.

Our variance of the NFs' AUC distributions was less than in the Adult Data experiment. We include figures and discussion in the Appendix 5.1.

4.2.1. Logistic Regression Results. Non-private LR results for both MIMIC-III prediction tasks reside in Table 3. Wang et al.'s LR used SciKit Learn while we use PyTorch.

To the best of our knowledge, the state-of-the-art for a differentially private LR model on MIMIC-III is given in [28]. They report LR model AUC for "low privacy" ($\varepsilon=3.5e5$, $\delta=1e-5$) and "high privacy" ($\varepsilon=3.5$, $\delta=1e-5$) on both ICU Mortality and Length of Stay tasks. Privacy of $\varepsilon>10$ is widely considered ineffective [21]; hence, the "low privacy" $\varepsilon=3.5e5$ is practically unreasonable but perhaps useful for investigating sensitivity of this parameter. Our replication of the same experiment produced LR models trained with DPSGD that greatly improve on this prior state-of-the-art. On ICU Mortality, Suriyakumar et al. [28] report 60% AUC for (3.5, 1e-5)-DP, whereas we are able to achieve 76% AUC for the same (3.5, 1e-5)-DP.

TABLE 2: Median AUC results on MIMIC-III Mortality and Length of Stay prediction experiments

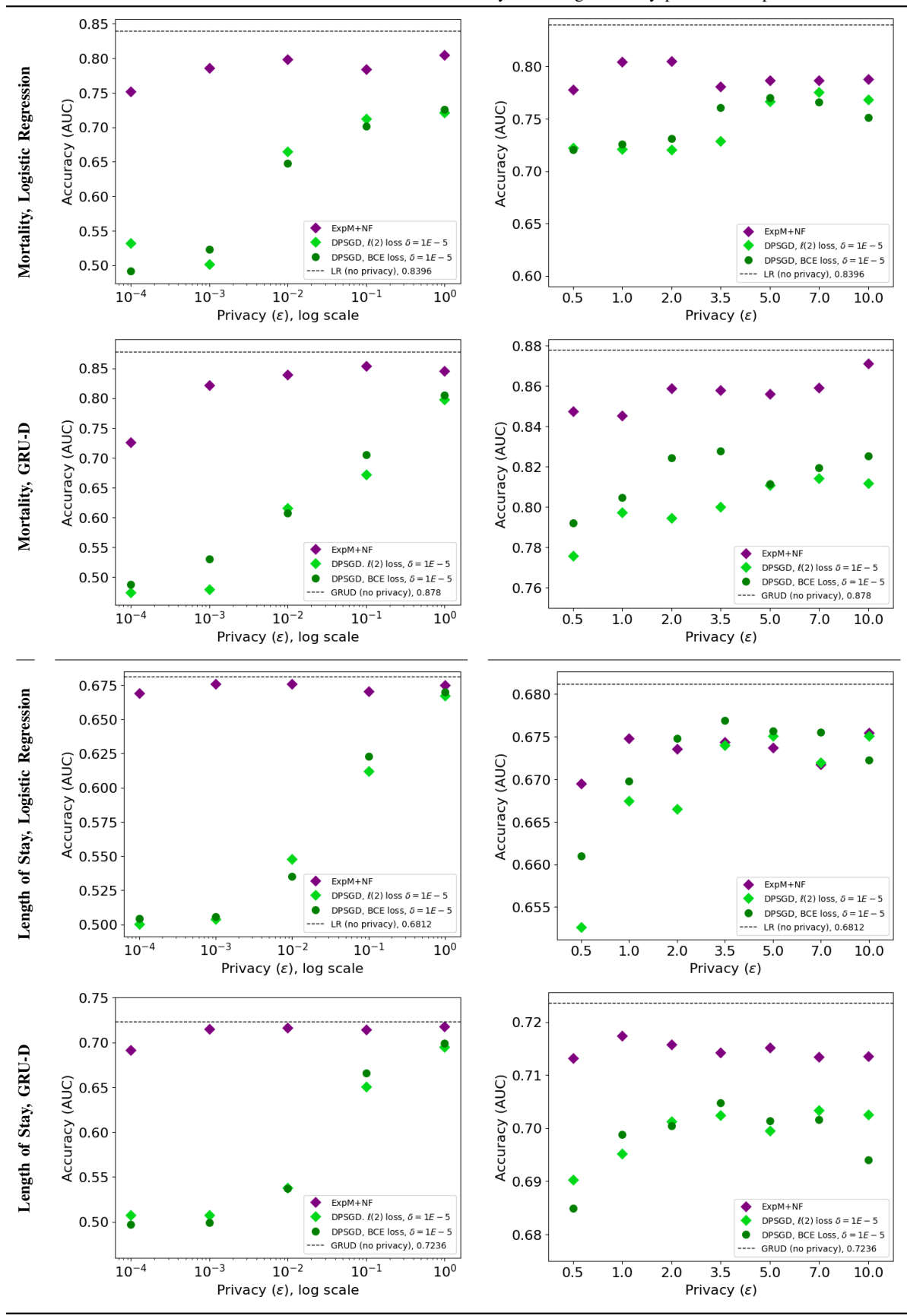


TABLE 3: AUC scores for non-private LR model results for this and prior works on MIMIC-III tasks. **Bold** results are best per task. Underlined are the best result in this work.

	[32]	[28]	$\ell(2)$ loss	BCE loss
ICU Mortality	.887	.82	<u>.839</u>	.83
Length of Stay	.716	.69	.675	.681

Our DPSGD implementations are able to achieve 72-76% AUC on this task for $0.5 \le \varepsilon \le 10$ and maintain AUC above 60% until $\varepsilon < 1\mathrm{e}{-1}$. For the Length of Stay task, Suriyakumar et al. [28] report 60% AUC for $(3.5, 1\mathrm{e}{-5})$ -DP, yet our models have 67% AUC for the same ε , which is only slightly below the non-private baseline. Again, we do not see an AUC below 60% until $\varepsilon < 1\mathrm{e}{-1}$. Much of this improvement can be attributed to using the PRV Accounting method, which allowed us to use much less noise to achieve the same level of privacy.

The ExpM+NF method outperforms these new state-of-the-art DPSGD results. As seen in Table 2, on the ICU Mortality task, ExpM+NF achieve 80.5% AUC (95% of the non-private AUC) for $\varepsilon=1$, and for $\varepsilon\geq 1\mathrm{e}-4$ results are above 89% of the non-private AUC (above 75% AUC). By comparison, DPSGD falls below 75% AUC, 89% of the non-private AUC, for $\varepsilon\leq 2$.

For the Length of Stay task, DPSGD surpasses ExpM+NF for $2 \le \varepsilon \le 7$, although all private models lie between 67.2–67.8% AUC, greater than 99% of the non-private AUC, $\varepsilon \ge 2$. Likely randomness due to the model initialization and noise in the hyperparameter search process may influence which model is slightly better/worse for any given $\varepsilon \ge 2$ as the results are so tight. However, a vast difference is again seen when the privacy is increased as ExpM+NF achieves over 97.5% of the non-private AUC for $\varepsilon \ge 1\mathrm{e}-4$. As was seen in the Adult Dataset experiment, there are times that for some smaller ε the ExpM+NF median AUC is greater than a nearby larger ε . Variations in the selected hyperparameters and initial starting conditions are the suspected cause.

4.2.2. GRU-D Results. Table 4 compares results of the GRU-D non-private baseline for previous works and ours, specifically including BCE vs $\ell(2)$ loss and with batch normalization vs. without. We see nearly identical results in our results for each prediction task across the two loss functions and with/without batch normalization, except for one instance, $\ell(2)$ loss with batch normalization is worse. GRU-D non-private baseline results of our method compared to previous works reside in Table 4. Our results are very close but slightly below Wang et al. [32], yet better than Suriyakumar et al. [28]. The gains in GRU-D's performance of ours and Wang et al.'s results may be due to differences in data or other implementation details. Specifically, our hyperparameter search found that a hidden size of about 35-40 performed best, which is much smaller than the 67 hidden size that [28] (and the original work of Che et al. [31]) used.

For the Length of Stay task, Suriyakumar et al. [28]

TABLE 4: AUC scores for non-private GRU-D model from this and prior works on MIMIC-III tasks. **Bold** results are best per task. <u>Underlined</u> results are best in this work per task. BN denotes batch normalization.

	[32]	[28]	$\ell(2$) loss	BC	E loss
	[32]	[28]	BN	No BN	BN	No BN
ICU Mortality	0.891	0.79	0.855	0.875	0.877	0.878
Length of Stay	0.733	0.67	0.721	0.724	0.722	0.722

report an AUC of 61% for GRU-D with (3.5, 1e-5)-DP. We reach 70% AUC with DPSGD for the same level of privacy. This is better than the AUC reported by Suriyakumar et al. [28] for both the non-private LR and GRU-D models and we are able to maintain an AUC greater than 65% for $\varepsilon > 1e-2$ with DPSGD. As we discussed in the prior section, much of the gains in AUC for GRU-D with DPSGD are likely due using the PRV Accounting method. Some of the gains could also be attributed to the same causes that provided the large gains we made for the non-private GRU-D model.

Suriyakumar et al. [28] show a sharp decrease in AUC when training GRU-D with DPSGD on ICU Mortality task, even in the "low privacy" case with $\varepsilon=3e5$. They report 59% AUC for this high ε and 53% AUC for the "strong privacy" case, (3.5, 1e-5)-DP, which is not much better than random guessing. Our DPSGD PRV implementation of GRU-D achieves median 82.7% AUC for (3.5, 1e-5)-DP using GRU-D on the Mortality prediction task. This is comparable to the best non-private LR model that we achieved, and is better than the performance [28] reported for non-private GRU-D. Our DPSGD results achieve AUC greater than 60% for each $\varepsilon>1e-2$ in this prediction task.

While the DPSGD results provide substantial gains on the prior state-of-the-art, the ExpM+NF method shows even further improvement. On the ICU Mortality task, we reach 87.1% AUC for $\varepsilon=10$, We maintain a median AUC greater than 82.5%, i.e., greater than 94% of the non-private AUC, for every $\varepsilon\geq 1\mathrm{e}-3$ we test. These results equal or surpass the best DPSGD AUC across all (ε,δ) that we explored. For the Length of Stay task, ExpM+NF exhibits 95.5% of the non-private AUC for all (AUC of at least 71%) for every $\varepsilon\geq 1\mathrm{e}-4$. This surpasses non-private results of Suriyakumr et al. [28]. Viewed another way, all ExpM+NF results for $\varepsilon=1\mathrm{e}-3$ surpass DPSGD results for any $\varepsilon!$

4.3. Training Times

In this section, we provide benchmark timings for training for our non-private, DPSGD and ExpM+NF implementations, and in the case of DPSGD, computing ε . We found that the best models for each of the different methods depended highly on the hyperparameter search results, and we only provide benchmarks for the best hyperparameters that were used for the test set. Specifically, the number of epochs and batch size will vary between the different implementations and in some cases the different privacy levels. As all our models are implemented in PyTorch, we use PyTorch's benchmark suite over ten runs on a single

		Logi	istic Regression		GRU-D			
Training	Loss	Training Time	Computing ε	Total	Training Time	Computing ε	Total	
Non- Private	ℓ(2) BCE	.87 ms 1.67 ms		.87 ms 1.67 ms	.84 ms .93 ms		.84 ms .93 ms	
DPSGD	ℓ(2) BCE	1.16 ms 1.56 ms	1.13 ms 1.2 ms	2.29 ms 2.76 ms	1.38 ms 1.46 ms	1.44 ms 1.34 ms	2.82 ms 2.8 ms	
ExpM+NF	RKL+ $\ell(2)$	1.65 ms	_	1.65 ms	1.71 ms	_	1.71 ms	

NVIDIA A100 80GB GPU and 128 CPUs with 2TB of shared RAM.

In Table 5 we report the mean timings for ICU Mortality Task for both LR and GRU-D models. For DPSGD and ExpM+NF, we additionally take the mean across the various privacy levels, noting that some ε may have hyperparameters that led it to take more or less time than this reported mean. For the non-private GRU-D implementation, we report mean training time with batch normalization which took less time. Timing results for Length of Stay are similar, and reside in the Appendix, Table 8, as well as more details on DPSGD timing in Tables 9, 10, and ExpM+NF training times in Table 7

In nearly every case, the non-private implementation takes the least total time, as is expected. In the case of the non-private BCE loss, the number of epochs and batch size were larger, likely attributing to the increased training time. LR and GRU-D models took similar amounts of time to train, likely to due the number of epochs required (GRU-D tended to need much fewer epochs than LR). ExpM+NF training time is more than DPSGD's training time, but when we add the additional time that DPSGD needs to compute ε , ExpM+NF performs better. There is little computational trade-off between DPSGD and ExpM+NF in these experiments. The innovation here is that our ExpM+NF code computes (and tracks gradients through) the $\ell(2)$ loss for the sampled parameters θ_i in parallel when computing the RKL loss for training the NF, rather than computing this sequentially.

5. Conclusion, Limitations, & Future Research

The fundamental observation driving this research is that DPSGD, the de facto method for differentially private ML, is wasteful by design in all but the relatively rare scenario when gradients are to be made public—noise is added to every gradient diminishing privacy with each epoch, and this entails the need for advanced composition theorems ensuring that $\delta > 0$. Our critical insight is two-fold: first, the well-established ExpM provides a tailored solution that bypasses these two problems, but the requisite distribution for ML applications is intractable; second, NF models provide a promising avenue for sampling from the ExpM distribution.

In this pioneering work, we find that ExpM+NF exhibits greater accuracy and privacy than the current SOTA in every experiment. Further, ExpM+NF achieves near optimal accuracy (> 93% of non-private training) for $\varepsilon \geq 5 \times 10^{-4}$

with $\delta=0$. As discussed by a recent survey on differentially private learning [21], ε in range [1,10] is expected with $\delta \approxeq 1/|X|$. ExpM+NF exhibits three to four orders of magnitude better privacy for similar and in most cases, better accuracy than DPSGD. Our overall conclusion is that ExpM+NF is superior in accuracy and privacy than DPSGD for training differentially private classification algorithms.

For all training methods, non-private, DPSGD, and ExpM+NF, results depended heavily on hyperparmeters, and we found ~100 hyperparmeter tuning runs were required to saturate our results. While we do not report the privacy loss due to hyperparameter tuning in this work, it does incur a privacy cost that ExpM+NF is well equipped to handle. ExpM+NF's ability to attain similar accuracy with orders of magnitude better privacy provides the privacy budget to implement the needed hyperparmeter tuning and still achieve a desirable privacy level.

Our implementations of DPSGD used the PRV accounting method, and our emperical results confirm its superiority over RDP accounting in both accurately estimating ε and the ability to handle $\varepsilon \leq 1\mathrm{e} - 1$.

Our results show that outlier NFs can produce bad results based on their randomized initializations. The increase in accuracy and privacy by ExpM+NF also affords a straightforward workaround, e.g., releasing ten models, each sampled from trained NFs with different starting seeds that are then used in a voting scheme.

We found that σ , the hyperparameter governing the variance of the NF's base distribution, has a large influence on results. Optimal σ found in hyperparameter searches tend to be larger for smaller ε , matching the intuition that the NF is more accurate if the base and output distributions' variance vary together. In future research, we suggest testing an NF that permits learning the base distribution's parameters during training.

The effect of using Sylvester flows (over planar flows) is increased expressiveness, but it does come at the cost of many more parameters in the NF model. For example, on the MIMIC-III ICU tasks we have dimension about d=2,500. With planar flows, the number of NF parameters needed to train an LR model is $(2d+1) \times$ number of flows, which is about 50,000 for 10 flows. With Sylvester flows the number of parameters is roughly $(d \times k + m^2 + m + d) \times$ the number of flows, where $k \leq d-1$ is how many Householder reflections to use and $m \leq d$ (for planar flows, m=1). If we use m=k=5 and 10 flows we

have about 150,000 NF parameters. Moving to the GRU-D models, we increase d to the $\mathcal{O}(50K)$, so the number of parameters explodes. Future research to understand the gain to accuracy-privacy vs the computational expense incurred by using more expressive NFs for ExpM+NF is needed.

In this work, bounding the sensitivity of the loss function, as is required for ExpM, was done by using $\ell(2)$ loss and the fact that our targets were bounded (binary, or one-hot). Even constrained to only $\ell(2)$ loss, ExpM+NF outperforms DPSGD with either BCE or $\ell(2)$ loss in nearly all experiments. Moving to a more general setting, especially regression with $\ell(2)$ loss or classification with other prominent loss functions, esp. log loss and KL divergence loss, will require custom sensitivity bounds for ExpM+NF (e.g., see [17]). Our results show that non-private and DPSGD training had similar results for both BCE and $\ell(2)$ loss in these classification tasks; on the other hand, the choice of loss function may prove a bigger effect on ExpM+NF's results since the sensitivity bounds has a direct effect on the variance of ExpM distribution.

In practice, randomness is produced from a pseudorandom algorithm, but differential privacy proofs follow from the assumption of true randomness. Prior works like [42] handle the use of pseudo-randomness by introducing a weaker computational differential privacy definition. We are unaware of mathematical treatment that seeks to estimate the effects of using pseudo-randomness on the privacy bound. For ExpM+NF, the psuedo-randomness comes from the NF's output distribution. It appears from the accuracy of our results that the NF is indeed approximating the correct density, (near optimal parameters are indeed found). Understanding how the privacy bound may be affected by the the NF approximation is a next step. Notably, training of the NF furnishes ample information on the discrepancieseach loss computation gives empirical KL divergence of the p_{ExpM} and the NF's output density that could be used to provide theorems that capture the difference into a quantifiable privacy guarantee. Further, using an NF that poorly approximates the ExpM distribution intuitively should furnish stronger privacy, as the algorithm is seemingly ignoring the training data.

How to craft an application of ExpM+NF to the federated setting and whether it can again push the SOTA is future research. Notably, one can theoretically derive DPSGD from using ExpM to sample gradients [11], so the most promising future direction of ExpM+NF in the federated setting is with federated model aggregation methods other than gradient aggregation and is a next step. Applications to popular federated techniques such as FedAve [43] and FedProx [44] should be straightforward.

Our initial, custom implementations were tested for training time against DPSGD and non-private training finding slightly faster training of ExpM+NF then DPSGD when time to compute the noise_multiplier for DPSGD is included. This shows that the method is computational feasible. While we provide our research code for reproducibility, professional engineering is needed for widespread adoption of ExpM+NF.

References

- [1] A. Yousefpour, I. Shilov, A. Sablayrolles, D. Testuggine, K. Prasad, M. Malek, J. Nguyen, S. Ghosh, A. Bharadwaj, J. Zhao, G. Cormode, and I. Mironov, "Opacus: User-friendly differential privacy library in PyTorch," <u>arXiv</u> preprint arXiv:2109.12298, 2021.
- [2] X. Zhang et al., "Adaptive privacy preserving deep learning algorithms for medical data," in Proceedings of the IEEE/CVF Winter Conference on Applications of Computer Vision, 2021. [Online]. Available: https://openaccess.thecvf.com/content/WACV2021/papers/Zhang_Adaptive_Privacy_Preserving_Deep_Learning_Algorithms_for_Medical_Data_WACV_2021_paper.pdf
- [3] S. Gao et al., "Classifying cancer pathology reports with hierarchical self-attention networks," <u>Artificial intelligence in</u> medicine, vol. 101, p. 101726, 2019.
- [4] M. Hassan, M. Rehmani, and J. Chen, "Differential privacy techniques for cyber-physical systems: a survey," <u>IEEE Communications Surveys & Tutorials</u>, vol. 22, no. 1, pp. 746–789, 2019.
- [5] M. U. Hassan <u>et al.</u>, "Differential privacy for renewable energy resources <u>based</u> smart metering," <u>Journal of Parallel</u> and Distributed Computing, vol. 131, pp. 69–80, 2019.
- [6] A. N. Dajani et al., "The modernization of statistical disclosure limitation at the u.s. census bureau," Presented at the September 2017 meeting of the Census Scientific Advisory Committee, 2017.
- Differential Apple Privacy Team. (2017) Learning with privacy scale. Accessed: 2023-07at [Online]. Available: https://machinelearning. apple.com/docs/learning-with-privacy-at-scale/ appledifferentialprivacysystem.pdf
- [8] U. Erlingsson, V. Pihur, and A. Korolova, "Rappor: Randomized aggregatable privacy-preserving ordinal response," in Proceedings of the 2014 ACM Conference on Computer and Communications Security, 2014, pp. 1054–1067.
- [9] B. Ding, J. Kulkarni, and S. Yekhanin, "Collecting telemetry data privately," in Advances in Neural Information Processing Systems 30, NIPS '17, 2017, pp. 3571–3580.
 [10] P. Xiong, T.-Q. Zhu, and X.-F. Wang, "A survey on dif-
- [10] P. Xiong, T.-Q. Zhu, and X.-F. Wang, "A survey on differential privacy and applications," Jisuanji Xuebao/Chinese Journal of Computers, vol. 37, no. 1, pp. 101–122, 2014.
- [11] F. McSherry and K. Talwar, "Mechanism design via differential privacy," in IEEE Symposium on Foundations of Computer Science, 2007, pp. 94–103.
- [12] A. Friedman and A. Schuster, "Data mining with differential privacy," in Proceedings of the 16th ACM SIGKDD international conference on Knowledge discovery and data mining, 2010, pp. 493–502.
- [13] M. Kapralov and K. Talwar, "On differentially private low rank approximation," in Proceedings of the twenty-fourth annual ACM-SIAM symposium on Discrete algorithms. SIAM, 2013, pp. 1395–1414.
- [14] S. A. Vinterbo, "Differentially private projected histograms: Construction and use for prediction," in <u>Joint European</u> Conference on Machine Learning and Knowledge Discovery in <u>Databases</u>. Springer, 2012, pp. 19–34.
- [15] S. P. Kasiviswanathan, H. K. Lee, K. Nissim, S. Raskhodnikova, and A. Smith, "What can we learn privately?" <u>SIAM</u> <u>Journal on Computing</u>, vol. 40, no. 3, pp. 793–826, <u>2011</u>. [Online]. Available: https://doi.org/10.1137/090756090
- [16] Z. Ji, Z. C. Lipton, and C. Elkan, "Differential privacy and machine learning: a survey and review," <u>arXiv preprint</u> <u>arXiv:1412.7584</u>, 2014.

- [17] K. Minami, H. Arai, I. Sato, and H. Nakagawa, "Differential privacy without sensitivity," in <u>Advances in Neural</u> Information Processing Systems 29, 2016.
- [18] J. P. Near and C. Abuah. (2022) Programming differential privacy. Accessed: 2023-09-15. [Online]. Available: https://programming-dp.com/
- [19] G. Papamakarios et al., "Normalizing flows for probabilistic modeling and inference," Journal of Machine Learning Research, vol. 22, no. 57, pp. 1–64, 2021.
- [20] M. Abadi et al., "Deep learning with differential privacy," in Proceedings of the 2016 ACM SIGSAC conference on computer and communications security, 2016.
- [21] N. Ponomareva, H. Hazimeh, A. Kurakin, Z. Xu, C. Denison, H. B. McMahan, S. Vassilvitskii, S. Chien, and A. G. Thakurta, "How to dp-fy ML: a practical guide to machine learning with differential privacy," vol. 77, 2023, pp. 1113–1201.
- [22] C. Dwork, "Sequential composition of differential privacy," Theory of Cryptography, pp. 222–232, 2007.
- [23] ——, "Advanced composition of differential privacy," in Proceedings of the 41st Annual ACM Symposium on Theory of Computing, 2010, pp. 436–445.
- [24] P. Kairouz, S. Oh, and P. Viswanath, "The composition theorem for differential privacy," <u>IEEE Transactions on</u> Information Theory, vol. 63, no. 6, pp. 4037–4049, 2017.
- [25] J. Dong, A. Roth, and W. Su, "Gaussian differential privacy," Journal of the Royal Statistical Society, 2021. [Online]. Available: https://par.nsf.gov/biblio/10215709
- [26] S. Gopi, Y. T. Lee, and L. Wutschitz, "Numerical composition of differential privacy," in Advances in Neural Information Processing Systems, M. Ranzato, A. Beygelzimer, Y. Dauphin, P. Liang, and J. W. Vaughan, Eds., vol. 34. Curran Associates, Inc., 2021, pp. 11631–11642. [Online]. Available: https://proceedings.neurips.cc/paper_files/paper/2021/file/6097d8f3714205740f30debe1166744e-Paper.pdf
- [27] A. Kurakin. (2022) Applying differential privacy to large scale image classification. Accessed: 2023-07-25. [Online]. Available: https://ai.googleblog.com/2022/02/ applying-differential-privacy-to-large.html
- [28] V. M. Suriyakumar, N. Papernot, A. Goldenberg, and M. Ghassemi, "Chasing your long tails: Differentially private prediction in health care settings," in <u>Proceedings of the 2021 ACM Conference on Fairness, Accountability, and Transparency</u>, 2021, pp. 723–734.
- [29] Adult dataset. Accessed: 2023-07-25. [Online]. Available: https://archive.ics.uci.edu/ml/datasets/adult
- [30] A. E. W. Johnson et al., "MIMIC-III, a freely accessible critical care database," Scientific data, vol. 3, 2016.
- [31] Z. Che <u>et al.</u>, "Recurrent neural networks for multivariate time series with missing values," <u>Scientific reports</u>, vol. 8, no. 1, pp. 1–12, 2018.
- [32] S. Wang et al., "Mimic-extract: A data extraction, preprocessing, and representation pipeline for mimiciii," in Proceedings of the ACM conference on health, inference, and learning, 2020. [Online]. Available: https://github.com/MLforHealth/MIMIC_Extract
- [33] C. Dwork and A. Roth, "The algorithmic foundations of differential privacy," <u>Found. Trends Theor. Comput. Sci.</u>, vol. 9, no. 3-4, pp. 211–407, 2014.
- [34] S. Neel, A. Roth, G. Vietri, and Z. S. Wu, "Differentially private objective perturbation: Beyond smoothness and convexity," ArXiv, vol. abs/1909.01783, 2019. [Online]. Available: https://api.semanticscholar.org/CorpusID:202537581
- [35] D. Rezende and S. Mohamed, "Variational inference with

- normalizing flows," in <u>International Conference on Machine</u> Learning, 2015.
- [36] R. Van Den Berg et al., "Sylvester normalizing flows for variational inference," in 34th Conference on Uncertainty in Artificial Intelligence, 2018.
- [37] X. Sun and C. Bischof, "A basis-kernel representation of orthogonal matrices," <u>SIAM</u> journal on matrix analysis and applications, vol. 16, no. 4, pp. 1184–1196, 1995.
- [38] D. Dua and C. Graff, "UCI machine learning repository," 2017. [Online]. Available: http://archive.ics.uci.edu/ml
- [39] "Codebase Opacus," https://opacus.ai/, accessed: 2023-07-25.
- [40] A. Yousefpour, I. Shilov, A. Sablayrolles et al., "Opacus: User-friendly differential privacy library in PyTorch," in NeurIPS Workshop Privacy in Machine Learning, 2021.
- NeurIPS Workshop Privacy in Machine Learning, 2021.
 [41] MIMIC-extract github repository. Accessed: 2023-05-25. [Online]. Available: https://github.com/MLforHealth/MIMIC_Extract
- [42] I. Mironov, O. Pandey, O. Reingold, and S. Vadhan, "Computational differential privacy," in <u>Annual International</u> Cryptology Conference. Springer, 2009, pp. 126–142.
- [43] B. McMahan, E. Moore, D. Ramage, S. Hampson, and B. A. y Arcas, "Communication-efficient learning of deep networks from decentralized data," in <u>Artificial intelligence</u> and statistics. PMLR, 2017, pp. 1273–1282.
- [44] T. Li, A. K. Sahu, M. Zaheer, M. Sanjabi, A. Talwalkar, and V. Smith, "Federated optimization in heterogeneous networks," Proceedings of Machine learning and systems, vol. 2, pp. 429–450, 2020.

Appendix

5.1. ExpM+NF AUC Distributions for MIMIC Experiments

In this section we provide ExpM+NF box plots for the MIMIC III Experiments. Figure 4 and Figure 5 show results for logistic regression models trained with ExpM+NF on ICU Mortality and Length of Stay tasks, respectively. For the first several privacy levels (decreasing at a logithmic rate), we can see that there are very few anomalous or bad starts, likely because the hyperparameters found were robust to these starting conditions. As the privacy level gets below 1e-4, we begin to see wide variations in how well the NFs perform. In this particular experiment, we do not begin to see median AUC below 60% until $\varepsilon=1-6$.

The results for GRU-D models trained on ICU Mortality are given in Figure 6 and GRU-D models trained on Length of Stay in Figure 7. Again, we see that for the first several privacy levels (decreasing logarithmically), there are very few anomalous starts. As we approach 1e-4, we begin to see more poor starts as the privacy level begins to affect performance.

While outlier NFs can occur, MIMIC III had far fewer than the Adult Dataset Experiment (see Figure 3) especially for $\varepsilon > 1\mathrm{e}{-4}$. This shows that some of the bad random initialization may also be dataset dependent. Overcoming these anomalous starts, when they do appear, can be handled by, e.g., releasing ten sampled models that are used in a voting scheme for slight privacy cost.

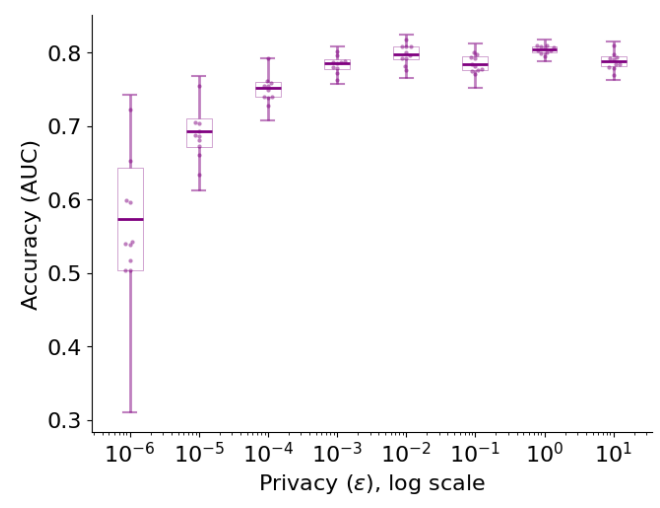


Figure 4: ICU Mortality Logistic Regression results, for each ε value, ten NF models are trained and used to produce 1,000 samples each from the ExpM distribution. We present box plots of the 10,000 resulting classifiers' AUC values. For each NF model's 1,000 samples we compute the mean AUC, which are overlayed as dots.

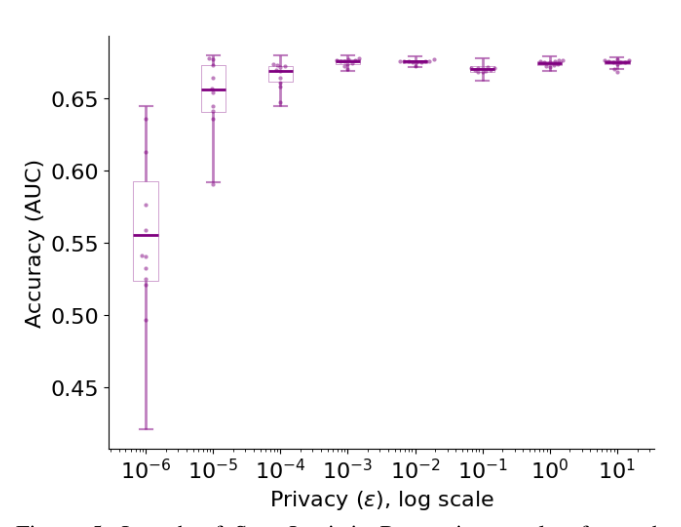


Figure 5: Length of Stay Logistic Regression results, for each ε value, ten NF models are trained and used to produce 1,000 samples each from the ExpM distribution. We present box plots of the 10,000 resulting classifiers' AUC values. For each NF model's 1,000 samples we compute the mean AUC, which are overlayed as dots.

5.2. Visualizing NF AUC Distributions

Our NFs produce densities in a high dimensional feature space; hence, we cannot easily visualize them. In, Figure 8, we plot the densities of a few NF models' AUC values from our experiments. We can see empirically the known trend that variance of our NF densities are increasing as privacy increases. Most are sharply unimodal.

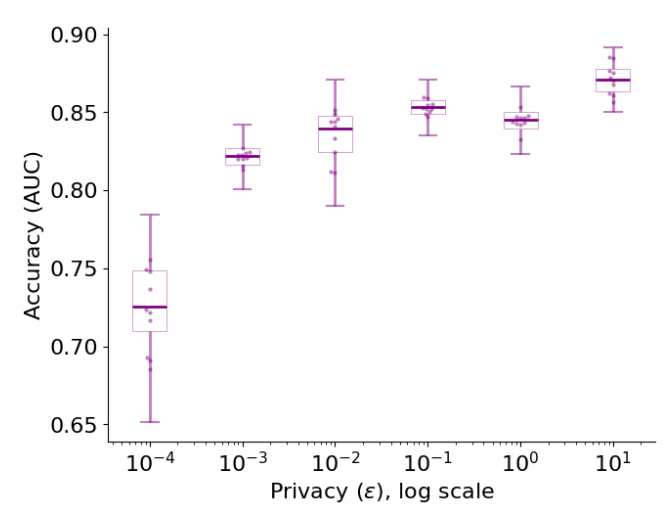


Figure 6: ICU Mortality GRU-D results, for each ε value, ten NF models are trained and used to produce 1,000 samples each from the ExpM distribution. We present box plots of the 10,000 resulting classifiers' AUC values. For each NF model's 1,000 samples we compute the mean AUC, which are overlayed as dots.

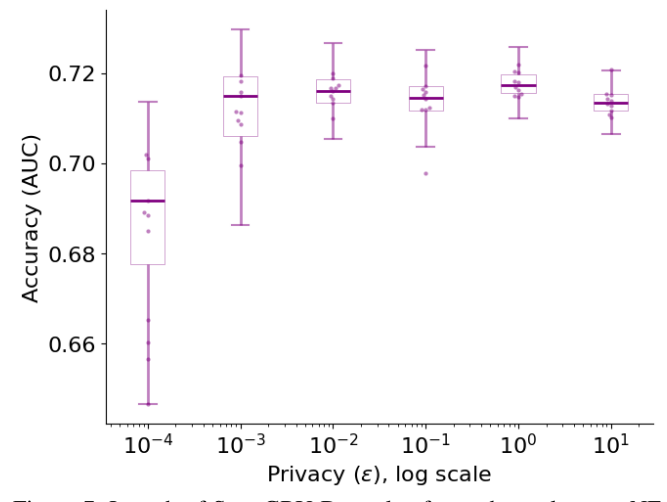


Figure 7: Length of Stay GRU-D results, for each ε value, ten NF models are trained and used to produce 1,000 samples each from the ExpM distribution. We present box plots of the 10,000 resulting classifiers' AUC values. For each NF model's 1,000 samples we compute the mean AUC, which are overlayed as dots.

5.3. RDP Accountant vs PRV Accountant

As DPSGD is so widely used, we provide the privacy estimates of using both the PRV and RDP accounting methods for our GRU-D DPSGD experiment in Table 6. For $\varepsilon>0.1$, the RPD Accounting method over estimates ε between 0.05-2.8. An important observation is that there appears to be a lower limit for the RDP Accounting method, showing that $\varepsilon>0.1$ even when the PRV Accountant is able to obtain $\varepsilon<0.1$.

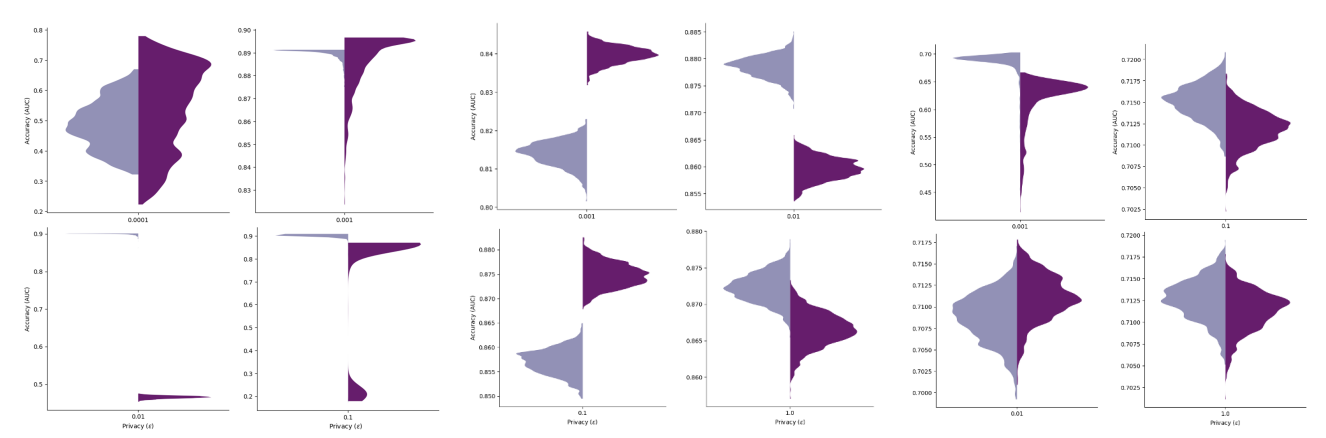


Figure 8: Each quad's subfigure provides violin plots depicting two (of ten) densities of NF models' AUC for four values of ε . Note the changing y scale. **Left quad** is from Adult Data LR model, **middle & right quads** are from MIMIC3 Length of Stay and Mortality prediction tasks, respectively, both with GRU-D model.

TABLE 6: DPSGD PRV vs. RDP Accountant Results for GRU-D model on ICU Mortality with $\delta=1\mathrm{e}-5$

		$\ell(2)$ 1	Loss		BCE Loss				
Target ε	Steps	noise_multplier	PRV ε	RDP ε	Steps	noise_multplier	PRV ε	RDP ε	
0.0001	4764	10240.0	0.0001 ± 0.0001	0.1029	6552	10240.0	0.0001 ± 0.0001	0.1029	
0.001	5820	320.0	0.0009 ± 0.0001	0.1029	7820	380.0	0.0009 ± 0.0001	0.1029	
0.01	873	25.156	0.0099 ± 0.0001	0.1034	3498	45.938	0.01 ± 0.0001	0.1034	
0.1	4368	6.172	0.0999 ± 0.001	0.1354	9372	7.109	0.0999 ± 0.001	0.1355	
0.5	2832	1.074	0.4969 ± 0.005	0.7866	3070	1.484	0.4986 ± 0.005	0.5571	
1.0	4370	0.889	0.9918 ± 0.01	1.3874	8904	1.328	0.9945 ± 0.01	1.0797	
2.0	4260	0.709	1.9903 ± 0.01	2.655	7176	0.854	1.9998 ± 0.01	2.3053	
3.5	3176	0.605	3.4961 ± 0.01	4.357	6678	0.688	3.4931 ± 0.01	4.1271	
5.0	2808	0.571	4.9985 ± 0.01	6.0285	3328	0.546	4.9963 ± 0.01	6.0799	
7.0	2107	0.511	6.9959 ± 0.01	8.3801	4720	0.502	6.9973 ± 0.01	8.371	
10.0	2709	0.474	9.9969 ± 0.01	11.7963	3834	0.457	9.9907 ± 0.01	11.8117	

5.4. Training Times

This section provides more detailed training time results. Table 5 reports the mean timings for ICU Mortality Task for both logistic regression and GRU-D models. For DPSGD and ExpM+NF, we additionally take the mean across the various privacy levels, noting that some ε may have hyperparameters that led it to take more or less time than this reported mean. For the non-private GRU-D implementation, we report mean training time without batch normalization which took less time.

Table 9 and Table 10 provide more detail on the mean time for each privacy level for DPSGD. We report mean time to compute privacy and the noise_multiplier but note that in practice only one of those would be needed. Interestingly, the privacy level itself does not seem to have much influence in the time it will take to train or compute ε , rather other hyperparameters are likely more influential.

Table 7 reports mean training times for ExpM+NF for each privacy level for the MIMIC III tasks. Much like DPSGD, we can see that the privacy level ε has little influence on how long training will take.

TABLE 7: ExpM+NF Mean Training Times in milliseconds (ms)

	ICU :	ICU Mortality		h of Stay
ε	LR	GRU-D	LR	GRU-D
0.0001	1.92	2.02	0.87	2.13
0.001	1.90	2.12	1.83	1.1
0.01	1.82	1.93	2.22	1.78
0.1	1.87	1.72	1.88	2.01
0.5	1.84	2.08	2.16	1.92
1.0	1.69	1.58	1.87	.93
2.0	1.73	2.05	1.02	1.92
3.5	1.11	1.29	1.79	2.54
5.0	1.83	1.90	1.00	1.48
7.0	1.79	1.20	2.06	1.96
10.0	1.78	1.97	1.87	2.1

TABLE 8: Length of Stay Benchmark Timing Results

		Logi	istic Regression		GRU-D			
Task	Loss	Training Time	Computing ε	Total	Training Time	Computing ε	Total	
Non- Private	ℓ(2) BCE	1.57 ms 1.51 ms		1.57 ms 1.51 ms	.81 ms 1.46 ms	<u>-</u> -	.81 ms 1.46 ms	
DPSGD	ℓ(2) BCE	1.41 ms 1.36 ms	1.36 ms 1.3 ms	2.77 ms 2.63 ms	1.8 ms 1.67 ms	1.5 ms 1.76 ms	3.3 ms 3.45 ms	
ExpM+NF	$RKL+\ell(2)$	1.74 ms	_	1.74 ms	1.81 ms	_	1.81 ms	

TABLE 9: DPSGD Length of Stay Benchmark Timing Results in Milliseconds (ms)

Model	Loss	Target ε	Mean Train Time	Mean Compute Time noise_multplier	Mean Compute Time ε (PRV)
		0.0001	1.66	0.85	1.86
		0.001	1.61	0.96	1.72
		0.01	1.0	1.56	0.9
		0.1	1.0	1.61	1.71
		0.5	1.06	1.43	0.89
	$\ell(2)$	1.0	1.73	1.52	1.87
		2.0	1.56	1.38	0.9
		3.5	1.30	1.82	0.94
		5.0	1.29	1.42	1.74
		7.0	1.76	2.09	0.83
		10.0	1.57	1.97	1.64
		0.0001	1.83	2.02	2.02
b		0.001	1.13	1.31	1.8
LogisticRegression		0.01	1.44	0.83	0.87
		0.1	1.77	1.87	1.63
		0.5	0.97	1.44	0.88
	BCE	1.0	0.83	1.37	0.96
		2.0	0.87	1.36	1.01
		3.5	1.65	1.96	1.2
		5.0	1.77	1.66	0.96
		7.0	1.86	1.79	1.56
		10.0	0.89	0.82	1.47
		0.0001	1.82	1.43	1.45
		0.001	1.87	1.87	1.81
		0.01	1.90	1.62	1.59
		0.1	1.76	1.06	2.09
		0.5	2.01	1.83	0.87
	$\ell(2)$	1.0	1.65	1.93	0.91
	()	2.0	1.77	1.78	1.31
		3.5	1.72	1.62	1.73
		5.0	2.09	1.98	1.99
١		7.0	1.59	1.40	0.90
		10.0	1.65	1.18	1.92
		0.0001	1.47	1.68	2.20
		0.001	1.95	1.92	1.82
		0.01	1.61	1.83	2.02
		0.1	1.66	1.42	2.22
		0.5	1.36	1.51	2.03
	BCE	1.0	1.93	1.64	1.11
	202	2.0	1.55	1.95	1.81
		3.5	1.98	2.01	1.60
		5.0	1.23	1.54	1.73
		7.0	1.73	0.96	0.88
		10.0	1.95	2.06	1.99

TABLE 10: DPSGD ICU Mortality Benchmark Timing Results in milliseconds (ms)

model	loss	target ε	Mean Train Time	Mean Compute noise_multplier	Mean Compute ε (PRV)
		0.0001	2.86	1.74	0.89
		0.001	0.81	1.96	0.85
		0.01	1.76	1.89	0.83
		0.1	1.63	1.65	0.86
		0.5	1.66	0.97	1.70
	$\ell(2)$	1.0	1.01	1.33	1.76
		2.0	0.83	1.36	0.85
Ę		3.5	0.82	1.72	0.87
sic		5.0	1.37	0.80	0.96
Se .		7.0	0.87	1.76	1.91
LogisticRegression		10.0	1.17	1.72	0.95
stic]		0.0001	1.88	1.79	1.92
igi		0.001	1.63	0.78	1.69
ĭ		0.01	1.44	1.11	1.50
		0.1	1.42	0.79	0.87
		0.5	1.98	1.61	0.91
	BCE	1.0	1.91	1.38	0.89
		2.0	1.63	1.43	1.78
		3.5	1.18	1.86	0.93
		5.0	1.05	1.32	0.91
		7.0	1.29	0.80	0.95
		10.0	1.77	2.79	0.92
		0.0001	1.13	1.85	1.23
		0.001	1.37	0.83	1.69
		0.01	1.68	1.64	1.73
		0.1	0.97	1.06	2.02
		0.5	0.88	1.77	1.05
	$\ell(2)$	1.0	1.85	1.79	1.50
	,	2.0	1.49	1.56	0.90
		3.5	1.60	1.46	1.28
		5.0	0.83	1.84	0.90
Ω		7.0	1.74	0.78	1.64
GRU-D		10.0	1.71	1.01	1.95
GF		0.0001	1.34	3.02	1.27
		0.001	1.89	1.14	0.87
		0.01	1.17	1.23	0.88
		0.1	0.83	1.09	0.92
		0.5	1.34	1.73	1.37
	BCE	1.0	1.06	0.92	1.97
		2.0	1.96	1.86	1.63
		3.5	1.01	1.89	0.88
		5.0	1.75	1.47	2.01
		7.0	2.44	1.75	0.89
		10.0	1.37	1.94	2.12